



Ptk7-Deficient Mice Have Decreased Hematopoietic Stem Cell Pools as a Result of Deregulated Proliferation and Migration

Anne-Catherine Lhoumeau, Marie-Laure Arcangeli, Maria de Grandis, Marilyn Giordano, Jean-Christophe Orsoni, Frédérique Lembo, Florence Bardin, Sylvie Marchetto, Michel Aurrand-Lions, Jean-Paul Borg

► To cite this version:

Anne-Catherine Lhoumeau, Marie-Laure Arcangeli, Maria de Grandis, Marilyn Giordano, Jean-Christophe Orsoni, et al.. Ptk7-Deficient Mice Have Decreased Hematopoietic Stem Cell Pools as a Result of Deregulated Proliferation and Migration. *Journal of Immunology*, 2016, 10.4049/jimmunol.1500680 . hal-01306950

HAL Id: hal-01306950

<https://hal.science/hal-01306950>

Submitted on 26 Apr 2016

HAL is a multi-disciplinary open access archive for the deposit and dissemination of scientific research documents, whether they are published or not. The documents may come from teaching and research institutions in France or abroad, or from public or private research centers.

L'archive ouverte pluridisciplinaire **HAL**, est destinée au dépôt et à la diffusion de documents scientifiques de niveau recherche, publiés ou non, émanant des établissements d'enseignement et de recherche français ou étrangers, des laboratoires publics ou privés.

***Ptk7* deficient mice have decreased Hematopoietic Stem Cell pools as a result of
deregulated proliferation and migration**

Anne-Catherine Lhoumeau^{1,2,3,4}, Marie-Laure Arcangeli^{2,3,4,5*}, Maria De Grandis^{2,3,4,5},
Marilyn Giordano^{1,2,3,4}, Jean-Christophe Orsoni^{1,2,3,4}, Frédérique Lembo^{1,2,3,4}, Florence
Bardin^{2,3,4,5}, Sylvie Marchetto^{1,2,3,4}, Michel Aurrand-Lions^{2,3,4,5} and Jean-Paul Borg^{1,2,3,4\$}

¹CRCM, Cell Polarity, Cell Signaling and Cancer “Equipe labellisée Ligue Contre le
Cancer”, Inserm, U1068, Marseille, F-13009, France; ²Institut Paoli-Calmettes, Marseille,
F-13009, France; ³CNRS, UMR7258 Marseille, F-13009, France; ⁴Aix-Marseille Univ, F-
13284, Marseille, France ; ⁵CRCM, Junctional Adhesion Molecules in Host/Tumor
Interactions, Inserm, U1068, Marseille, F-13009, France.

* Present address: INSERM U967, iRCM-CEA, Fontenay-aux-Roses, France

^{\$}Corresponding author: jean-paul.borg@inserm.fr

Tel : 33 4 86 97 72 01; Fax : 33 4 86 97 74 99

Keywords: PTK7, planar cell polarity, hematopoietic stem cells, homing

Running title: Role of the polarity protein PTK7 in murine haematopoiesis.

25 **Abstract**

26 Hematopoietic Stem Cells (HSCs) located in adult bone marrow or fetal liver in mammals
27 produce all cells from the blood system. At the top of the hierarchy are long-term HSCs
28 endowed with lifelong self-renewal and differentiation properties. These features are
29 controlled through key microenvironmental cues and regulatory pathways such as Wnt
30 signaling. We have previously shown that PTK7, a tyrosine kinase receptor involved in
31 planar cell polarity (PCP), plays a role in epithelial Wnt signaling. However, its function in
32 hematopoiesis has remained unexplored. Here we show that PTK7 is expressed by
33 hematopoietic stem and progenitor cells (HSPCs) with the highest protein expression level
34 found on HSCs. Taking advantage of a *Ptk7* deficient mouse strain, we demonstrate that
35 loss of *Ptk7* leads to a diminished pool of HSCs, but does not affect *in vitro* or *in vivo*
36 hematopoietic cell differentiation. This is correlated with increased quiescence and reduced
37 homing capacities of *Ptk7* deficient HSPCs, unravelling novel and unexpected functions for
38 planar cell polarity pathways in HSC fate.

39

40

41 **Introduction**

42 Hematopoiesis is a biological process consisting on the production of all blood cell
43 types from hematopoietic stem cells (HSCs) located in the bone marrow (BM) of adult
44 mammals. Fetal hematopoiesis occurs in different sites, particularly in the liver, during its
45 earliest phases. Long term hematopoietic stem cells (LT-HSCs) are characterized by their
46 capacity to provide lifelong reconstitution of all blood cell lineages after transplantation
47 into lethally irradiated recipients, whereas short term HSCs (ST-HSCs) do so for only 8-10
48 weeks.

49 In the mouse, LT-HSCs belong to the LSK cell compartment defined by the
50 Lineage^{-low} Scd1⁺c-Kit⁺ phenotype irrespectively of their fetal liver (FL) or adult bone
51 marrow (BM) origin. Additional markers known as SLAM (Signal Lymphocytes Activating
52 Molecules) can further subdivide this compartment (1)(2). Indeed, CD150⁺CD48⁻ LSK have
53 been shown to contain around 40% of HSCs with long-term reconstitution potential in BM
54 as well as in FL (3).

55 Hematopoiesis is a highly controlled multi-step process that relies on complex
56 interaction networks involving cell surface receptors, growth factors, and adhesion
57 molecules expressed by HSCs and their environment (4)(5)(6)(7)(8). Because HSCs
58 generate mature hematopoietic cells, including immune cells, their replacement must be
59 adjusted to homeostatic or stress conditions such as infections, inflammation or blood loss,
60 and their expansion must be controlled to avoid exhaustion. This control is made possible
61 by the coordinated regulation of quiescence, self-renewal, and differentiation through
62 appropriate signals delivered by functional BM niches (9). HSCs are retained in these BM
63 niches by cell surface molecules endowed with adhesive and/or signalling functions
64 expressed by HSCs. These receptors belong to different protein families: integrins (VLA-4)
65 (10), Immunoglobulin superfamily (Ig Sf) adhesion molecules (6) (11), G Protein Coupled

66 Receptors (CXCR4)(12), or tyrosine kinase receptors (TIE2, c-Kit)(13)(14)(15) interacting
67 with ligands present within the BM microenvironment (16). Discovery of novel molecules
68 implicated in this multi-step program is of particular importance to embrace its complexity,
69 develop new strategies aiming at the regeneration of damaged hematopoietic tissues and to
70 understand hematopoietic diseases.

71 PTK7 is a planar cell polarity (PCP) receptor belonging to the Immunoglobulin
72 Superfamily (Ig Sf) and playing important roles during development (17)(18). PCP is
73 controlled by a non-canonical Wnt pathway, organizes polarization of many epithelial
74 tissues and organs within the plane and drives cell migration and cell intercalation of non-
75 epithelial cells such as mesenchymal cells (19)(20). *Ptk7* deficient mouse embryos show all
76 signs of typical PCP defects such as severe tube neural and abdomen closure defect with
77 secondary development abnormalities (21). PTK7 is a type I protein composed of seven Ig
78 loops in its extracellular region, a transmembrane domain, an intracellular region with a
79 tyrosine kinase domain (17)(18)(22)(23). While PTK7 is catalytically inactive, the
80 cytoplasmic domain containing the tyrosine kinase domain is mandatory for receptor
81 function *in vitro* and *in vivo* (24)(25)(26)(27). Both extracellular and intracellular domains
82 of PTK7 can be released from the plasma membrane following the sequential cleavage of
83 the receptor by membrane type 1-matrix metalloproteinase (MT1-MMP)/ADAM-17, and γ -
84 secretase, interfering with its PCP and promigratory activities (24)(28)(29).

85 We have recently found that PTK7 expression is not restricted to epithelial cells.
86 Indeed, PTK7 is expressed at the cell surface of human hematopoietic progenitors and acute
87 myeloid leukemia (AML) patient blast cells. Overexpression of the PCP protein leads to
88 increased cell survival and cell migration of leukemic cells and confers a poor prognosis to
89 patients independently of other risk factors (27). Similar conclusions were recently drawn

from studies done in chronic lymphocytic leukemia in which a set of PCP proteins is upregulated (30).

Although functions of canonical and non-canonical Wnt pathways have been extensively studied in hematopoiesis (for review see (31)(32)(33)), the role of PTK7 has never been explored in this process. In the present study, we have thus addressed the function of PTK7 in physiological hematopoiesis using a mouse model deficient for *ptk7* expression. Using flow cytometry, we first mapped expression of PTK7 on HSCs and progenitors. As PTK7 deficient mice die perinatally, we then studied function of PTK7 in fetal hematopoiesis and revealed a decreased number of HSPCs in FL of *Ptk7* deficient mice. Although HSC differentiation was not affected, we found a dramatic decrease in proliferation and migration properties of *Ptk7* deficient HSPCs that reveal novel unexpected functions for this planar cell polarity molecule.

Methods

Mice

C57BL/6 and C57BL/6-CD45.1 were purchased from Janvier Laboratory and Charles River Laboratories, respectively. All mice used for transplantation experiments are 6 to 12 weeks old. Lethal irradiation was done with an X-ray irradiator (X-RAD® 160 X-Ray, PXi) using a single dose of 8Gy.

PTK7 gene-trap mice were obtained by injection of gene-trap ES XST087 (Bays Genomics, USA) in E3.5 blastocyst from C57BL/6 mouse. Chimeric mice were back-crossed with B6 mice for seven generations to obtain homogenous genetic background for experiments. All mice were housed and maintained under specific pathogen-free condition. E14.5 and 15.5 were used in all FL experiments. All animal experiments were performed in agreement with the French Guidelines for Animal Handling.

Genotyping

Genotyping of adult mice and embryos was performed by genomic PCR using the following pairs of primers: 5'- ACGTCACTGGAGAGGAAGTCCGCAG-3' and 5'- GATCGAAGCAGGTCCTGTGGTCCT-3' for wild type allele and 5'- TTGTGAAGTGGAGGCTCCGGACC-3' and 5'- CGATCTTCCTGAGGCCGATACTGTC-3' for gene trap insertion allele.

Flow cytometry and cell sorting

For the analysis of hematopoietic stem/progenitor cells in FLs, FLs were dissected from E14.5 embryos and single cell suspension was made in phosphate-buffered saline (PBS)-2% Fetal Calf Serum (FCS).

For analysis of hematopoietic stem/progenitor cells in BM, thymus or blood cells obtained from adult mice were suspended in PBS-2% FCS. For BM and thymus, cells were filtered using 70 µm cell strainer (BDFalcon) and lysis of red blood cells was done using ACK lysis buffer (0.15 M NH₄Cl, 10mM KHCO₃, 0.1mM Na₂EDTA, Life Technology) for 2 min at room temperature. Cells were spun and resuspended in PBS-2%FCS +/- 0.125mM EDTA for staining. For blood samples, red blood cell lysis was done after staining using BD FACS Lysing buffer solution (BD Biosciences) following manufacturer instructions.

For flow cytometry analysis and cell sorting, cells were stained with monoclonal antibodies purchased from Ebiosciences or Biolegend against the following molecules: B220 (clone 6B2), CD3 (145-2C11), CD4 (RM4-5), CD8 (53-6.7), CD11b/Mac-1 (M1/70), CD11c (N418), CD16/32 (93), CD19 (6D5), CD24 (M1/69), CD34 (RAM34), CD45 (30F11), CD45.1/Ly5.1 (A20), CD45.2/Ly5.2 (104), CD48 (HM48-1), CD49b (DX5), CD49d (R1-2), CD117/c-Kit (2B8 and/or ACK2), CD135 (A2F10), CD150 (TC15-12F12.2), F4/80 (BM8), Gr1 (RB6-8C5), Sca-1 (D7), Ter-119. Antibody human PTK7 and glycophorin A (11E4B-7-6) were purchased from Miltenyi biotech and Beckman Coulter, respectively.

All experiments were done by multicolour parametrics analysis using FITC, PE, APC, PE-Cy7, APC-Cy7, PerCPCy5.5, AlexaFluor700, AlexaFluor594, Pacific blue, PE-Cy5, Q-dot 605 fluorochroms or spectral equivalents. Commercial antibodies were used either directly conjugated or biotinylated. For mouse PTK7 expression, polyclonal rabbit antibody raised against recombinant PTK7-Fc was used in the experiments. For detection of interesting antigen, PE or APC-conjugated goat-anti-rabbit (Jackson ImmunoResearch Laboratories) were used as secondary antibodies. To exclude lineage positive cells, streptavidin conjugated with Alexa A594 (Invitrogen) or Pacific blue (Ebiosciences) were used. Irrelevant isotype-matched antibodies were used as controls. Cells were stained 20 minutes at 4°C and rinsed in PBS-2% FCS solution. Viability marker (vivid dye, Invitrogen) was

added in last staining in PBS solution. Stained cells were analysed by LSR II SORP (laser 405, 488, 561, and 633; BD Bioscience) or sorted by ARIA III (BD Bioscience). LSK cell populations were purified by cell sorting using a FACS-ARIA with > 95% purity. Results were analyzed using BD-DIVA Version 6.1.2 software (BD Biosciences) or FlowJo Version 7.6.2 (TreeStar) software.

Homing experiments

E14.5 embryos were sacrificed and were immediately genotyped. FL cells from wild type or gene trap mice were suspended, counted and stained with cell tracker calcein AM and calcein red-orange (Invitrogen), respectively, according manufacturer instructions. Cells were mixed at 1/1 ratio and $4 \cdot 10^6$ total cells were injected through retro-orbital vein in previously irradiated (8 Gy) mice. 12h after injection, mice were sacrificed and blood, bone marrow, spleen, liver and thymus samples were analysed for fluorescent cells.

Transplantation assays

For LSK sorting, FL cells (CD45.2+) were labelled for lineage positive (lin+) cells with following biotinylated primary rat antibodies (lineage mix): CD3, CD4, CD8, CD19, B220, DX5, TER-119, GR-1, CD11c. Lin+ cells were depleted by magnetic separation using anti-rat Ig coated magnetic beads (DynaBeads, Lifetechnology). Lin^{Neg} cells were also stained and sorted by FACS according to the phenotype Lin^{Neg}, CD45.2⁺, Kit⁺ and Sca-1⁺. CD45.1 mice were lethally irradiated and grafted with 1000 or 400 CD45.2⁺ LSK cells through the retro-orbital vein along with $1 \cdot 10^5$ total BM recipient cells to allow short term reconstitution and mice survival. Recipient mice survival was followed and BM engraftment was examined by monitoring donor (CD45.2⁺ cells) and host cell (CD45.1⁺ cells) frequency in

the blood. After lethal irradiation, mice were maintained on water containing neomycin sulfate 1g/500mL for 2 weeks.

Serial transplantation assay

Lethally irradiated (8 Gy) mice (C57Bl/6, CD45.1) received 3×10^6 total fetal liver cells (first transplantation) or BM total cells (next transplantations). BM engraftment was monitored as described above.

Competition assay

Lethally irradiated (8 Gy) mice (C57Bl/6, CD45.1) received 2×10^6 total FL cells from CD45.2 PTK7^{-/-} mutant embryos and 2×10^6 total FL cells from CD45.1⁺CD45.2⁺ PTK7^{+/+} embryos, issues from crossing of C57Bl/6, CD45.1 and C57Bl/6, CD45.2. Plugs are obtained the same day. BM engraftment was examined by monitoring frequency of CD45.2⁺ cells from PTK7 mutant donors and CD45.1⁺CD45.2⁺ cells from wild type donor, excluding CD45.1⁺ cells from host cells, in the blood. After lethal irradiation, mice were maintained on water containing neomycin sulfate 1g/500mL for 2 weeks.

Cell cycle analysis and apoptosis analysis

FL progenitors were enriched as previously described and stained with cKit-APC-eFluor750, CD150-APC, Sca-1-PerCP-Cy5.5, and CD48-PECy7. The biotin-conjugated lineage combination was revealed with AlexaFluor 594-streptavidin (Invitrogen). For cell cycle analysis, after extracellular staining, cells were permeabilized, fixed, and stained with anti-Ki67-FITC MoAb (BD Biosciences) and DAPI as previously described (34). For apoptosis analysis, cells were stained with PE-annexine V to evaluate annexine V externalization (BD biosciences) and DAPI.

201

202 *In vitro methylcellulose assays*

203 For methylcellulose colony assays, FL or BM cells suspensions were prepared in Iscove
204 modified Dulbecco medium (IMDM) supplemented with 2% FBS. $3 \cdot 10^4$ cells of FL or
205 $1 \cdot 10^5$ cells of BM were seeded in Methocult M3434 (containing rmSCF 50 ng/mL, rmIL-3
206 10ng/mL, rhIL-6 10ng/mL, and EPO 3U/mL) (from Stem Cell Technologies, Grenoble,
207 France) in 35 mm dishes accordingly to manufacturer's instructions. All assays were done
208 in triplicated. Colonies (>30 cells) were counted after 13 days of incubation at 37°C , 5%
209 CO_2 and humidified atmosphere.

210

211 *Adhesion assays*

212 MS5 stromal cells were plated on 96-well flat bottom plates, at a concentration of $5 \cdot 10^3$
213 cells/well 1 day before the assay. MS5 is a stromal cell line that has been generated by
214 irradiating adherent cells in long-term BM culture. Lin^{Neg} FL cells ($5 \cdot 10^5$) obtained as
215 previously described were cocultured for 2 hours with MS5 stromal cells. Plates were
216 washed 3 times with PBS and adherent cells were removed by strong pipetting in PBS
217 1.25mM EDTA 2% FCS. The phenotype of adherent cells was determined using anti-
218 CD117, Sca-1, CD150, CD48, and FITC-lineage mix to exclude any residual mature cells
219 contaminating the Lin^{Neg} preparation. Absolute numbers were measured using the HTS
220 coupled to the BD-LSR2 SORP (BD Bioscience).

221

222 *Migration assays*

223 Lin^{Neg} FL cells were enriched as previously described and suspended in Iscove modified
224 Dulbecco medium (IMDM) containing 2% of bovine serum albumine. About $2 \cdot 10^5$ cells in
225 75 μl were loaded in 5- μm pore Transwell system (Corning Life Sciences). The lower

chamber was filled with Serum free Media supplemented with the chemoattracting murine stromal-derived factor-1 (mSDF-1 α , 100 ng/mL, Peprotech). The same number of cells was plated in distinct wells to be used as control for migration. Plates were then incubated 4 hours at 37°C, 5% CO₂. All experiments were performed in duplicates. Cells were also stained using anti-CD117, Sca-1 and streptavidin coupled to Pacific Blue as described above. Absolute numbers were measured using the HTS coupled to the BD-LSR2 SORP (BD Bioscience) and the migration ratio was defined as the number of migrating cells between migration wells and control wells.

TF1 cell differentiation

Growth of the human erythroid/macrophage progenitor cell line TF1 is dependent on GM-CSF or IL3 and can be induced to differentiate in the presence of growth factors. TF1 cells were grown in IMDM medium supplemented with 5 ng/ml GM-CSF and supplemented with EPO (2 UI/ml) for erythroid differentiation. TF1 cells were infected by viral particles containing shRNA against PTK7 as previously described (27). A scramble non-targeting shRNA was used as a control. shRNA efficiency for PTK7 downregulation was controlled by flow cytometry before and at the end of experiments. TF1 cells were then differentiated in IMDM with 2 IU/ml EPO and without GM-CSF for a total of seven days as previously described (35). Erythroblastic differentiation was evaluated by glycophorin A expression.

Statistical analysis

Statistical significance was determined with nonparametric Mann-Whitney *U* test using Prism Version 5 software (Graphpad Software Inc).

Results

PTK7 is expressed on HSCs, myeloid progenitors, lymphoid and thymic progenitors

In a first approach, we studied PTK7 pattern of expression in adult murine hematopoietic cells. To this end, a rabbit polyclonal antibody generated against the extracellular region of PTK7 was used. This antibody recognizes mouse PTK7 endogenously expressed on endothelial and hematopoietic cells by FACS analysis in wild type but not *ptk7* deficient mice (Supplementary Fig. S1). Analysis of PTK7 expression in peripheral blood and in splenocytes revealed that none of the mature mouse leukocytes subsets (granulocytes, monocytes, B cells and T cells) expressed PTK7 to detectable level (Fig. 1A and data not shown). We next analysed PTK7 expression in murine BM hematopoietic progenitors using multiparametric flow cytometry and gating strategies described in Figure 1B. When LSK subsets were examined, PTK7 expression was found to be inversely correlated to differentiation stages with the highest expression on HSCs and multipotent progenitors (MPP) type 1 HSC-MPP1 (RFI=40), and intermediate expression on MPP2 (RFI=20) and MPP3-MPP4 (RFI=15) (Fig. 1C). More committed progenitors including common myeloid progenitors (CMP) and common lymphoid progenitors (CLP) expressed PTK7 at lower levels while the protein was almost undetectable on the surface of granulocyte-macrophage progenitor (GMP), and megakaryocyte-erythroid progenitor (MEP) (Fig. 1D). A similar phenotypic analysis was conducted on differentiating T cells isolated from the thymus. T cell progenitors do not express CD4 and CD8 markers and are called double negative (DN) cells before differentiation into double positive (DP) and single positive (SP) cells. Within the DN compartment, four thymic progenitor populations can be identified according to CD44 and CD25 expression from the most immature DN1 to the most mature DN4 subsets. PTK7 is expressed by the CD44+CD25- (DN1) population and expression is conserved

during thymic differentiation within the DN2, DN3 and DN4 subpopulations (Supplementary Fig. S2). PTK7 expression is also detected on DP thymocytes before becoming progressively lost at the SP stage. Altogether, these phenotypic analyses reveal that PTK7 expression is inversely correlated to hematopoietic differentiation with the highest expression found in HSCs. This suggests that PTK7 may play a role at this early stage of hematopoietic differentiation.

Ptk7^{-/-} embryos have a quantitative defect of hematopoietic stem cells

We next questioned the function of PTK7 in hematopoiesis. To this end, we generated a *Ptk7* deficient mouse strain using a gene-trapped ES cell available through the International Gene Trap Consortium. As expected from the previous description of *Ptk7* deficient strains, we observed a perinatal lethality due to profound developmental defects (21). *Ptk7^{-/-}* embryos harbour a severe phenotype with cranial neural tube closure defect, gastroschisis, kidney and forelimb abnormalities (Fig. 2A, 2B). Considering this dramatic phenotype, it was impossible to study adult hematopoiesis in these mice and we thus decided to study FL hematopoiesis. In FL, as well as in the BM, HSCs are comprised within the LSK cell compartment. Using the same gating strategy as in Figure 1, we analysed the consequences of PTK7 deficiency in the different LSK cell populations (Fig. 2C). We observed a 25% decrease of total cellularity at E14.5 in PTK7 deficient FL compared to wild type FL (Fig. 2D). However proportion of leucocytes (e.g. CD45⁺ cells) is equivalent between deficient and wild type FL (Fig. 2E) suggesting that the decrease in FL cellularity in *Ptk7^{-/-}* embryos is likely due to a global effect of *ptk7* deficiency on FL size. We next examined the hematopoietic progenitor compartment. A decrease of about 50% of LSK cell frequency was observed in *Ptk7* deficient FL compared to control FL (1.33% *Ptk7^{+/+}* and *+/+* LSK cells versus 0.67% *Ptk7^{-/-}* LSK cells) (Fig. 2F). In the different LSK cell populations, the

most affected one was the HSC-MPP1 subset (Fig. 2C and 2G). No significant difference in the frequency of MMP2 and MPP3-MPP4 subsets was observed in *Ptk7* deficient FL compared to wild type or heterozygous FL. When we examined the absolute number of the different subsets of hematopoietic progenitors, we noticed that all LSK subsets were affected by PTK7 deficiency. Indeed, there was a 68% decrease in the LSK cell absolute number in *Ptk7* deficient embryos compared to control embryos (Fig. 2H). The most dramatic decrease was observed in the HSC compartment. Indeed, there was up to 75% decrease in HSC number in *Ptk7*^{-/-} embryos compared to control one whereas there was around a 50% decrease in MPP2 and MPP3/4 cell numbers (Fig. 2I).

To assess the frequency of functional HSC in FL, we transplanted 1000 and 400 sorted LSK cells from *Ptk7*^{+/+} or *Ptk7*^{-/-} FL bearing the CD45.2 allele into two groups of lethally irradiated mice bearing the CD45.1 allele. As expected, all mice included in the group injected with 1000 LSK cells survived. However, with 400 injected cells, *Ptk7*^{+/+} FL LSK cells were able to reconstitute recipient mice between 2 and 12 weeks after injection whereas all mice except one injected with *Ptk7*^{-/-} LSK cells died within 6 weeks (Fig. 2J). We concluded that loss of PTK7 leads to a defect in functional HSC frequency. *In vitro* clonogenicity assays confirmed the defect in HSCs and early precursor frequency as we observed a twofold reduction in colony-forming units starting from 3.10⁴ total FL cells. (Fig. 2K).

320 *PTK7 deficient fetal liver cells are more quiescent than wild type fetal liver cells*

321 To determine if the absence of PTK7 could alter HSC quiescence, we performed cell cycle
322 phenotypic analysis of LSK FL cells using an antibody directed against Ki-67, a nuclear
323 marker to measure cell cycle, and DAPI to evaluate the DNA content (Fig. 3A). We found
324 that a greater proportion of HSCs and early progenitors were in G0 phase in *Ptk7* deficient
325 embryos as compared to control. Indeed, 56% of HSC-MPP1 cells were quiescent in *Ptk7*
326 deficient embryos with respect to 46% in control embryos (Fig. 3B). This significant
327 increase in quiescent cells was maintained throughout hematopoietic differentiation with
328 respectively 46% versus 39% and 19% versus 14% of the cells in G0 phase at the MMP2
329 and MPP3-MPP4 stages (Fig. 3B). To exclude that these unbalanced proportion of
330 quiescent cells was not due to selective apoptosis of cycling *Ptk7* deficient cells, we
331 analyzed the percentage of apoptotic cells in *Ptk7* deficient and control FL cells. We did not
332 observed a difference of apoptosis as measured by Annexin V staining between wild type
333 and mutant mice in total FL cells and LSK cells (Fig. 3C). These results demonstrate that
334 PTK7 delivers proliferative signals to HSCs but does not affect HSC survival.

336 *PTK7 deficient cells are able to reconstitute definitive hematopoiesis in recipient mice*

337 To investigate the functional capacity of *Ptk7* deficient HSCs, we generated chimeric mice
338 using FL cell transplantation. CD45.1 C57Bl/6 mice were lethally irradiated (8 Gy) and
339 then reconstituted with 3.10^6 total FL cells from *Ptk7* deficient or wild type FL embryos
340 (CD45.2). Reconstitution and chimerism were followed over time by monitoring the
341 frequency of donor cells (CD45.2) versus recipient cells (CD45.1) in the peripheral blood
342 of recipient mice (Fig. 4A). As expected, all recipient mice injected with control FL cells
343 were reconstituted between 2 and 12 weeks. The same results were obtained with PTK7
344 deficient FL cells demonstrating that in absence of any competition, *Ptk7* deficient HSCs

are able to reconstitute all mature hematopoietic lineages of lethally irradiated recipients (Fig. 4B-C). To investigate whether *Ptk7* deficiency could lead to more subtle hematopoietic defects, BM of chimeric mice was analyzed after twelve weeks. No significant difference was found in frequencies of mature and progenitor cells in the BM (Fig. 4E-F). In agreement with reconstitution experiments, *in vitro* differentiation assays showed that *Ptk7* deficient FL cells are able to give rise to all subtypes of colony forming units in the same proportion than control FL cells (Fig. 4G, left panel and supplementary Fig.S4). However, we observed fewer colonies generated by *Ptk7* deficient HSPC than by control cells (Fig. 4G, right panel). This is likely due to decreased cell cycle activity of *Ptk7* deficient HSPCs while the potential of differentiation is not affected. Since quiescence of HSCs could be correlated to loss of self-renewal (36), we then tested self-renewal capacities of *Ptk7* deficient HSCs by serial transplantation assays. Recipient CD45.1 mice were lethally irradiated and reconstituted with CD45.2 donor cells from wild type and mutant mice. The first injection was performed with 3.10^6 total FL cells. After 12 weeks, BM cells were harvested and 3.10^6 cells were then injected to a second lethally irradiated recipient. The same protocol was applied for the following transplantations. We monitored chimerism by flow cytometry analysis and obtained a very good reconstitution with about 95 to 100% of donor cells in BM for all transplantations (Fig. 4H). We also investigated erythroblastic reconstitution in mice and did not find any differences in term of hemoglobin level and red blood cell count (Supplementary Fig. S3A and S3B). *In vitro* differentiation using TF1 cells that are able to differentiate in response to EPO did not reveal any difference in the presence or absence of PTK7 (Supplementary Fig. S3C and S3D). We thus concluded that PTK7 is not required for hematopoietic differentiation.

To get further insights into PTK7 function in early hematopoiesis, we performed mixed chimera competition experiments. CD45.1 C57Bl/6 mice were lethally irradiated (8 Gy)

and then reconstituted with $2 \cdot 10^6$ total FL cells from *Ptk7* deficient (CD45.2) and $2 \cdot 10^6$ total FL cells from wild type FL embryos (CD45.2xCD45.1). Reconstitution and chimerism were followed over time by monitoring the frequency of *PTK7*^{-/-} cells (CD45.2) and *PTK7*^{+/+} (CD45.2⁺CD45.1⁺) versus recipient cells (CD45.1) in the peripheral blood of recipient mice. We did not observe significant differences at D30 and D60, but observed an advantage of *PTK7*^{-/-} cells at long term (>120 jours) (Fig. 5A). Since maintenance of quiescence is a stem cell property, we tested cell cycle activity of adult HSC in chimeric mice. Recipient CD45.1 mice were lethally irradiated and reconstituted with CD45.2 donor cells from wild type and mutant FL mice as previously described. We performed cell cycle analysis on hematopoietic progenitors more than 6 months post transplantation, when stable hematopoietic reconstitution is obtained. We confirmed that hematopoietic progenitors isolated from mice reconstituted with *PTK7* deficient cells are more quiescent than wild type counterparts (Fig. 5B and 5C). Clonogenic experiments confirmed that fewer colonies are generated by *Ptk7* deficient HSPC than by control from chimeric mice (Fig. 5D). These results suggest that *PTK7* is essential for quiescence independently of the microenvironment.

Homing and migration defects of Ptk7 deficient cells

Since we have previously described a pro-migratory function of *PTK7* in leukemic cell lines and because increased HSC quiescence may not be the unique cause of the functional defect of *Ptk7*^{-/-} HSCs (Fig. 2J), we decided to investigate the role of *PTK7* in hematopoietic homing. FL cells from several *Ptk7*^{-/-} or *Ptk7*^{+/+} embryos were pooled and stained separately with two different fluorescent trackers. Cells were injected according to a 1/1 ratio and mice were sacrificed 12h after injection. Analysis of homing was performed by flow cytometry (Fig. 6A-C). Although we observed comparable levels of residual

395 circulating cells regardless the PTK7 status in peripheral blood, *Ptk7* deficient cells had a
396 very poor capacity to home to the BM, spleen, liver, and thymus as compared to control
397 (Fig. 6D). Since homing defect can be explained by loss of cell adhesion to BM stromal
398 cells and/or by a defect of cell migration toward a chemoattractant, we tested these two
399 hypotheses. Adhesion of *Ptk7* deficient LSK cells on the murine MS5 stromal cell line was
400 not significantly different from control LSK cells (Fig. 7A). In contrast, we found a
401 decrease in spontaneous transmigration of *Ptk7* deficient FL cells as compared to control
402 cells in Boyden chamber assay (8% versus 5%, Fig. 7B). No effect was observed with
403 heterozygous FL cells. We also observed significant differences when the chemokine
404 SDF1 α was used as a chemoattractive molecule. Indeed, whereas 12% of control FL cells
405 migrated toward SDF1 α , only 8% of PTK7 deficient FL cells were able to do so (Fig. 7C).
406 Without chemoattractant, less than 5% of LSK cells migrated across the transwell
407 regardless the PTK7 status (Fig. 7D). When SDF1 α was used as a chemoattractive molecule,
408 a twofold decrease in LSK transmigration was observed for *Ptk7* deficient cells as
409 compared to control cells (20% versus 40%, Fig. 7E).

Discussion

Discovery of novel molecular pathways implicated in HSC maintenance is of particular interest to develop new strategies aiming at the regeneration of damaged hematopoietic tissues and to understand hematopoietic diseases such as leukemia. We have previously identified the cell polarity protein, PTK7, as a novel tyrosine kinase receptor overexpressed in acute myeloid leukemia (AML). High expression of PTK7 is correlated to poor prognosis and resistance to chemotherapeutic regimens (27). Recently, another study revealed that PTK7 is also upregulated in T acute lymphocytic leukemia (T-ALL)(37). In humans, we and others have evidenced that PTK7 expression is mostly restricted to normal early progenitors committed to myeloid and T lymphoid lineages.

In the present study, we show that PTK7 expression is similar between mouse and human systems. PTK7 is absent in mature blood cells and its expression in BM hematopoietic progenitors is inversely correlated with differentiation. The highest expression of PTK7 is found in HSC-MPP1 compartment. PTK7 expression is also conserved between mice and human when the thymic compartment is considered. PTK7 is easily detectable at the cell surface of CLP and immature DN and DP populations whereas its expression is lost in single positive CD4 or CD8 lymphocytes. These data correlate with results from other groups that demonstrated expression of PTK7 by recent thymic emigrants cells and thymocytes (38)(37).

In order to study the role of PTK7 in hematopoiesis, we generated *Ptk7* deficient mice using available gene-trapped ES cells. Our *Ptk7* deficient strain exhibited expected planar cell polarity defects as compared to another strain of mice issued from the same ES clone (21). Since these mutant mice cannot reach adulthood, functions of PTK7 were investigated in FL hematopoietic cells. The major hematopoietic phenotype of *Ptk7* deficient mice consists in increased quiescence of HSPCs and shrinkage of the FL HSPC pool. Although these

phenotypes may sound logical if one considers that less proliferation produces less cells, they are difficult to reconcile with loss of functional reconstitution observed when recipient mice are engrafted with limited numbers of LSK cells (Fig. 2J). Indeed, PTK7 is implicated in canonical and non-canonical Wnt pathway (17)(39), which are thought to be the guardians of the balance between HSC self-renewal and HSC differentiation (32). We have recently shown that PTK7 plays a role in canonical pathway downstream of Wnt3a suggesting that deficiency in PTK7 may mirror deficiency in Wnt3a (25). This would be consistent with results showing that Wnt3a deficiency leads to a reduction in the numbers of HSPCs in the FL but would not fit with the reduced reconstitution capacity observed in secondary transplantation assays of Wnt3a deficient cells which is not observed with *Ptk7* deficient cells (40). Alternatively, it may well be that PTK7 controls non-canonical pathway through interaction with Wnt ligands (41) (42). In this way, Wnt5a antagonizes Wnt3a-mediated canonical signaling and increases quiescence of HSCs (43). This occurs through activation of the small Rho GTPase Cdc42 that increases HSC polarity (44)(45). Such a function of PTK7 in Wnt5a-mediated non-canonical pathway would fit with the planar cell polarity function of PTK7 and with altered homing and migrating properties of *Ptk7* deficient cells that likely depend on small Rho GTPase activation. Some studies show that PTK7 regulates the balance between Wnt canonical and non-canonical pathways by interacting with Dishevelled (26)(46), ROR2 (42)(47), β -catenin (25) and LRP6 (39). We unsuccessfully tried to identify downstream pathways that could be regulated by Ptk7 in HSCPs using a candidate gene/protein approach. We also looked at gene expression differences between Ptk7 knock-out and control hematopoietic cells using unbiased gene expression profiling. Although we identified differences (data not shown), we could not find obvious Gene Ontology enrichments or pathways that could be experimentally tested. Further studies will be needed to unravel how Ptk7 functions in HSPCs.

In our model of FL hematopoietic cells, we confirmed the role of PTK7 in cell migration and found a new role of this protein in cell homing to hematopoietic organs and in the control of cell proliferation. This observation confirms our previous data obtained from human leukemia samples (27) can be linked with already described functions of PTK7 in cell migration and in metastatic dissemination. Indeed, we and others have found that PTK7 expression on various cancer cells is linked with higher metastasis potential (27)(29)(48)(49). Recently, we also described a poor prognosis of PTK7 expression in colon cancer cells linked with higher metastatic events (50). In addition, our data show for the first time that PTK7 is involved in the regulation of hematopoietic and stem and progenitors cell (HSPC) cycle. Lack of PTK7 expression increases quiescence and enhances the long term repopulating potential after six months, while a trend toward decreased chimerism is observed after one or two months. This could reflect the dual function of PTK7 loss of expression in decreasing short term homing to the bone marrow and increasing long term establishment of hematopoiesis. Alternatively, it may well be that homing assay performed with total liver cells reveals a constitutive promigratory function of PTK7, in contrast to long term engraftment reflecting bone marrow micro-environmental signaling through PTK7 in HSCs. Similar complex mechanisms of cell cycle regulation and differential homing of mature cells versus HSPCs homing to the bone marrow have also been attributed to CXCR4 (51) (52) (53) (54). Whether PTK7 and CXCR4 signaling share more in common remains to be addressed. In conclusion, PTK7 overexpression in immature blasts cells of acute myeloid leukemia has been associated to bad prognosis, early relapse and chemotherapeutic resistance and a recent study shows that PTK7 can be used as a stem cell marker of colon cancer stem cells (27)(55). Taken together, all these data form a set of arguments to involve PTK7 expression in stem cells including cancer stem cells but also to prove a functional role of PTK7 in stem cell biology. We think that these new data

on PTK7 involvement on cell cycle are very promising to understand molecular mechanisms of leukemia/cancer development.

Altogether, our results report a novel unexpected function for the planar cell polarity molecule PTK7 in the crosstalk between expansion of HSPC compartment and HSPC migration. This opens new avenue for manipulation of HSC fate using agonists or antagonists of PTK7.

For Peer Review. Do not distribute. Destroy after use.

494

495 **Acknowledgments**

496 We thank Patrick Gibier, Patrick Garzino and Annaëlle Legrand from the animal facility of
497 CRCM.

498

499 **Author contribution**

500 A.-C.L designed experiments, wrote the paper, performed all experiments and generated
501 deficient mice; M.D.G, M.G., F.L., F.B., S.M. helped to perform experiments; J.-C.O.
502 generated deficient mice; M-L.A., M.A-L, J-P.B. designed experiments and wrote the
503 paper.

504

505 **Disclosure of potential conflicts of interest**

506 All authors declare no conflict of interest.

507

508 **References**

- 509 1. Kiel, M. J., O. H. Yilmaz, T. Iwashita, O. H. Yilmaz, C. Terhorst, and S. J. Morrison.
510 2005. SLAM family receptors distinguish hematopoietic stem and progenitor cells and
511 reveal endothelial niches for stem cells. *Cell* 121: 1109–1121.
- 512 2. Oguro, H., L. Ding, and S. J. Morrison. 2013. SLAM family markers resolve functionally
513 distinct subpopulations of hematopoietic stem cells and multipotent progenitors. *Cell Stem*
514 *Cell* 13: 102–116.
- 515 3. Kim, I., S. He, O. H. Yilmaz, M. J. Kiel, and S. J. Morrison. 2006. Enhanced purification
516 of fetal liver hematopoietic stem cells using SLAM family receptors. *Blood* 108: 737–744.
- 517 4. Golan, K., Y. Vagima, A. Ludin, T. Itkin, S. Cohen-Gur, A. Kalinkovich, O. Kollet, C.
518 Kim, A. Schajnovitz, Y. Ovadya, K. Lapid, S. Shvitiel, A. J. Morris, M. Z. Ratajczak, and
519 T. Lapidot. 2012. S1P promotes murine progenitor cell egress and mobilization via S1P1-
520 mediated ROS signaling and SDF-1 release. *Blood* 119: 2478–2488.
- 521 5. Lapidot, T., P. Goichberg, K. Lapid, A. Avigdor, and O. Kollet. 2007. The endosteum
522 region keeps human leukemic stem cells alive. *Cell Stem Cell* 1: 483–484.
- 523 6. Arcangeli, M.-L., V. Frontera, F. Bardin, E. Obrados, S. Adams, C. Chabannon, C.
524 Schiff, S. J. C. Mancini, R. H. Adams, and M. Aurrand-Lions. 2011. JAM-B regulates
525 maintenance of hematopoietic stem cells in the bone marrow. *Blood* 118: 4609–4619.
- 526 7. Ooi, A. G. L., H. Karsunky, R. Majeti, S. Butz, D. Vestweber, T. Ishida, T. Quertermous,
527 I. L. Weissman, and E. C. Forsberg. 2009. The adhesion molecule esam1 is a novel
528 hematopoietic stem cell marker. *Stem Cells Dayt. Ohio* 27: 653–661.
- 529 8. Winkler, I. G., V. Barbier, B. Nowlan, R. N. Jacobsen, C. E. Forristal, J. T. Patton, J. L.
530 Magnani, and J.-P. Lévesque. 2012. Vascular niche E-selectin regulates hematopoietic stem
531 cell dormancy, self renewal and chemoresistance. *Nat. Med.* 18: 1651–1657.
- 532 9. Morrison, S. J., and D. T. Scadden. 2014. The bone marrow niche for haematopoietic
533 stem cells. *Nature* 505: 327–334.
- 534 10. Papayannopoulou, T., C. Craddock, B. Nakamoto, G. V. Priestley, and N. S. Wolf.
535 1995. The VLA4/VCAM-1 adhesion pathway defines contrasting mechanisms of
536 lodgement of transplanted murine hemopoietic progenitors between bone marrow and
537 spleen. *Proc. Natl. Acad. Sci. U. S. A.* 92: 9647–9651.
- 538 11. Hidalgo, A., F. Sanz-Rodríguez, J. L. Rodríguez-Fernández, B. Albella, C. Blaya, N.
539 Wright, C. Cabañas, F. Prósper, J. C. Gutierrez-Ramos, and J. Teixidó. 2001. Chemokine
540 stromal cell-derived factor-1 α modulates VLA-4 integrin-dependent adhesion to
541 fibronectin and VCAM-1 on bone marrow hematopoietic progenitor cells. *Exp. Hematol.*
542 29: 345–355.
- 543 12. Ara, T., K. Tokoyoda, T. Sugiyama, T. Egawa, K. Kawabata, and T. Nagasawa. 2003.
544 Long-term hematopoietic stem cells require stromal cell-derived factor-1 for colonizing
545 bone marrow during ontogeny. *Immunity* 19: 257–267.
- 546 13. Arai, F., A. Hirao, M. Ohmura, H. Sato, S. Matsuoka, K. Takubo, K. Ito, G. Y. Koh,
547 and T. Suda. 2004. Tie2/angiopoietin-1 signaling regulates hematopoietic stem cell
548 quiescence in the bone marrow niche. *Cell* 118: 149–161.
- 549 14. McCulloch, E. A., L. Siminovich, J. E. Till, E. S. Russell, and S. E. Bernstein. 1965.
550 The cellular basis of the genetically determined hemopoietic defect in anemic mice of
551 genotype Sl-Sld. *Blood* 26: 399–410.
- 552 15. Barker, J. E. 1994. Sl/Sld hematopoietic progenitors are deficient in situ. *Exp. Hematol.*
553 22: 174–177.
- 554 16. Wilson, A., and A. Trumpp. 2006. Bone-marrow haematopoietic-stem-cell niches. *Nat.*
555 *Rev. Immunol.* 6: 93–106.

17. Lhoumeau, A.-C., F. Puppo, T. Prébet, L. Kodjabachian, and J.-P. Borg. 2011. PTK7: a cell polarity receptor with multiple facets. *Cell Cycle Georget. Tex* 10: 1233–1236.
18. Peradziriyi, H., N. S. Tolwinski, and A. Borchers. 2012. The many roles of PTK7: a versatile regulator of cell-cell communication. *Arch. Biochem. Biophys.* 524: 71–76.
19. Angers, S., and R. T. Moon. 2009. Proximal events in Wnt signal transduction. *Nat. Rev. Mol. Cell Biol.* 10: 468–477.
20. Sebbagh, M., and J.-P. Borg. 2014. Insight into planar cell polarity. *Exp. Cell Res.* .
21. Lu, X., A. G. M. Borchers, C. Jolicœur, H. Rayburn, J. C. Baker, and M. Tessier-Lavigne. 2004. PTK7/CCK-4 is a novel regulator of planar cell polarity in vertebrates. *Nature* 430: 93–98.
22. Jung, J. W., A. R. Ji, J. Lee, U. J. Kim, and S. T. Lee. 2002. Organization of the human PTK7 gene encoding a receptor protein tyrosine kinase-like molecule and alternative splicing of its mRNA. *Biochim. Biophys. Acta* 1579: 153–163.
23. Mossie, K., B. Jallal, F. Alves, I. Sures, G. D. Plowman, and A. Ullrich. 1995. Colon carcinoma kinase-4 defines a new subclass of the receptor tyrosine kinase family. *Oncogene* 11: 2179–2184.
24. Na, H.-W., W.-S. Shin, A. Ludwig, and S.-T. Lee. 2012. The cytosolic domain of protein-tyrosine kinase 7 (PTK7), generated from sequential cleavage by a disintegrin and metalloprotease 17 (ADAM17) and γ -secretase, enhances cell proliferation and migration in colon cancer cells. *J. Biol. Chem.* 287: 25001–25009.
25. Puppo, F., V. Thomé, A.-C. Lhoumeau, M. Cibois, A. Gangar, F. Lembo, E. Belotti, S. Marchetto, P. Lécine, T. Prébet, M. Sebbagh, W.-S. Shin, S.-T. Lee, L. Kodjabachian, and J.-P. Borg. 2011. Protein tyrosine kinase 7 has a conserved role in Wnt/ β -catenin canonical signalling. *EMBO Rep.* 12: 43–49.
26. Shnitsar, I., and A. Borchers. 2008. PTK7 recruits dsh to regulate neural crest migration. *Dev. Camb. Engl.* 135: 4015–4024.
27. Prebet, T., A.-C. Lhoumeau, C. Arnoulet, A. Aulas, S. Marchetto, S. Audebert, F. Puppo, C. Chabannon, D. Sainty, M.-J. Santoni, M. Sebbagh, V. Summerour, Y. Huon, W.-S. Shin, S.-T. Lee, B. Esterni, N. Vey, and J.-P. Borg. 2010. The cell polarity PTK7 receptor acts as a modulator of the chemotherapeutic response in acute myeloid leukemia and impairs clinical outcome. *Blood* 116: 2315–2323.
28. Golubkov, V. S., A. V. Chekanov, P. Cieplak, A. E. Aleshin, A. V. Chernov, W. Zhu, I. A. Radichev, D. Zhang, P. D. Dong, and A. Y. Strongin. 2010. The Wnt/planar cell polarity protein-tyrosine kinase-7 (PTK7) is a highly efficient proteolytic target of membrane type-1 matrix metalloproteinase: implications in cancer and embryogenesis. *J. Biol. Chem.* 285: 35740–35749.
29. Golubkov, V. S., N. L. Prigozhina, Y. Zhang, K. Stoletov, J. D. Lewis, P. E. Schwartz, R. M. Hoffman, and A. Y. Strongin. 2014. Protein-tyrosine pseudokinase 7 (PTK7) directs cancer cell motility and metastasis. *J. Biol. Chem.* 289: 24238–24249.
30. Kaucká, M., K. Plevová, S. Pavlová, P. Janovská, A. Mishra, J. Verner, J. Procházková, P. Krejčí, J. Kotasková, P. Ovesná, B. Tichý, Y. Brychtová, M. Doubek, A. Kozubík, J. Mayer, S. Pospíšilová, and V. Bryja. 2013. The planar cell polarity pathway drives pathogenesis of chronic lymphocytic leukemia by the regulation of B-lymphocyte migration. *Cancer Res.* 73: 1491–1501.
31. Kokolus, K., and M. J. Nemeth. 2010. Non-canonical Wnt signaling pathways in hematopoiesis. *Immunol. Res.* 46: 155–164.
32. Malhotra, S., and P. W. Kincade. 2009. Wnt-related molecules and signaling pathway equilibrium in hematopoiesis. *Cell Stem Cell* 4: 27–36.

33. Florian, M. C., K. J. Nattamai, K. Dörr, G. Marka, B. Uberle, V. Vas, C. Eckl, I. Andrä, M. Schiemann, R. A. J. Oostendorp, K. Scharffetter-Kochanek, H. A. Kestler, Y. Zheng, and H. Geiger. 2013. A canonical to non-canonical Wnt signalling switch in haematopoietic stem-cell ageing. *Nature* 503: 392–396.
34. Wilson, A., G. M. Oser, M. Jaworski, W. E. Blanco-Bose, E. Laurenti, C. Adolphe, M. A. Essers, H. R. Macdonald, and A. Trumpp. 2007. Dormant and self-renewing hematopoietic stem cells and their niches. *Ann. N. Y. Acad. Sci.* 1106: 64–75.
35. Wang, F., J. Travins, B. DeLaBarre, V. Penard-Lacronique, S. Schalm, E. Hansen, K. Straley, A. Kernysky, W. Liu, C. Gliser, H. Yang, S. Gross, E. Artin, V. Saada, E. Mylonas, C. Quivoron, J. Popovici-Muller, J. O. Saunders, F. G. Salituro, S. Yan, S. Murray, W. Wei, Y. Gao, L. Dang, M. Dorsch, S. Agresta, D. P. Schenkein, S. A. Biller, S. M. Su, S. de Botton, and K. E. Yen. 2013. Targeted inhibition of mutant IDH2 in leukemia cells induces cellular differentiation. *Science* 340: 622–626.
36. Fleming, H. E., V. Janzen, C. Lo Celso, J. Guo, K. M. Leahy, H. M. Kronenberg, and D. T. Scadden. 2008. Wnt signaling in the niche enforces hematopoietic stem cell quiescence and is necessary to preserve self-renewal in vivo. *Cell Stem Cell* 2: 274–283.
37. Jiang, G., M. Zhang, B. Yue, M. Yang, C. Carter, S. Z. Al-Quran, B. Li, and Y. Li. 2012. PTK7: a new biomarker for immunophenotypic characterization of maturing T cells and T cell acute lymphoblastic leukemia. *Leuk. Res.* 36: 1347–1353.
38. Haines, C. J., T. D. Giffon, L.-S. Lu, X. Lu, M. Tessier-Lavigne, D. T. Ross, and D. B. Lewis. 2009. Human CD4⁺ T cell recent thymic emigrants are identified by protein tyrosine kinase 7 and have reduced immune function. *J. Exp. Med.* 206: 275–285.
39. Bin-Nun, N., H. Lichtig, A. Malyarova, M. Levy, S. Elias, and D. Frank. 2014. PTK7 modulates Wnt signaling activity via LRP6. *Dev. Camb. Engl.* 141: 410–421.
40. Luis, T. C., B. A. E. Naber, W. E. Fibbe, J. J. M. van Dongen, and F. J. T. Staal. 2010. Wnt3a nonredundantly controls hematopoietic stem cell function and its deficiency results in complete absence of canonical Wnt signaling. *Blood* 116: 496–497.
41. Peradziryi, H., N. A. Kaplan, M. Podleschny, X. Liu, P. Wehner, A. Borchers, and N. S. Tolwinski. 2011. PTK7/Otk interacts with Wnts and inhibits canonical Wnt signalling. *EMBO J.* 30: 3729–3740.
42. Martinez, S., P. Scerbo, M. Giordano, A. M. Daulat, A.-C. Lhoumeau, V. Thomé, L. Kodjabachian, and J.-P. Borg. 2015. The PTK7 and ROR2 Protein Receptors Interact in the Vertebrate WNT/Planar Cell Polarity (PCP) Pathway. *J. Biol. Chem.* 290: 30562–30572.
43. Nemeth, M. J., L. Topol, S. M. Anderson, Y. Yang, and D. M. Bodine. 2007. Wnt5a inhibits canonical Wnt signaling in hematopoietic stem cells and enhances repopulation. *Proc. Natl. Acad. Sci. U. S. A.* 104: 15436–15441.
44. Florian, M. C., K. Dörr, A. Niebel, D. Daria, H. Schrezenmeier, M. Rojewski, M.-D. Filippi, A. Hasenberg, M. Gunzer, K. Scharffetter-Kochanek, Y. Zheng, and H. Geiger. 2012. Cdc42 activity regulates hematopoietic stem cell aging and rejuvenation. *Cell Stem Cell* 10: 520–530.
45. Schlessinger, K., E. J. McManus, and A. Hall. 2007. Cdc42 and noncanonical Wnt signal transduction pathways cooperate to promote cell polarity. *J. Cell Biol.* 178: 355–361.
46. Wehner, P., I. Shnitsar, H. Urlaub, and A. Borchers. 2011. RACK1 is a novel interaction partner of PTK7 that is required for neural tube closure. *Dev. Camb. Engl.* 138: 1321–1327.
47. Podleschny, M., A. Grund, H. Berger, E. Rollwitz, and A. Borchers. 2015. A PTK7/Ror2 Co-Receptor Complex Affects Xenopus Neural Crest Migration. *PloS One* 10: e0145169.

48. Shin, W.-S., J. Kwon, H. W. Lee, M. C. Kang, H.-W. Na, S.-T. Lee, and J. H. Park. 2013. Oncogenic role of protein tyrosine kinase 7 in esophageal squamous cell carcinoma. *Cancer Sci.* 104: 1120–1126.
49. Jin, J., H. S. Ryu, K. B. Lee, and J.-J. Jang. 2014. High expression of protein tyrosine kinase 7 significantly associates with invasiveness and poor prognosis in intrahepatic cholangiocarcinoma. *PloS One* 9: e90247.
50. Lhoumeau, A.-C., S. Martinez, J.-M. Boher, G. Monges, R. Castellano, A. Goubard, M. Doremus, F. Poizat, B. Lelong, C. de Chaisemartin, F. Bardin, P. Viens, J.-L. Raoul, T. Prebet, M. Aurrand-Lions, J.-P. Borg, and A. Gonçalves. 2015. Overexpression of the Promigratory and Prometastatic PTK7 Receptor Is Associated with an Adverse Clinical Outcome in Colorectal Cancer. *PloS One* 10: e0123768.
51. Cashman, J., I. Clark-Lewis, A. Eaves, and C. Eaves. 2002. Stromal-derived factor 1 inhibits the cycling of very primitive human hematopoietic cells in vitro and in NOD/SCID mice. *Blood* 99: 792–799.
52. Broxmeyer, H. E., L. Kohli, C. H. Kim, Y. Lee, C. Mantel, S. Cooper, G. Hangoc, M. Shaheen, X. Li, and D. W. Clapp. 2003. Stromal cell-derived factor-1/CXCL12 directly enhances survival/antiapoptosis of myeloid progenitor cells through CXCR4 and G(alpha)i proteins and enhances engraftment of competitive, repopulating stem cells. *J. Leukoc. Biol.* 73: 630–638.
53. Foudi, A., P. Jarrier, Y. Zhang, M. Wittner, J.-F. Geay, Y. Lecluse, T. Nagasawa, W. Vainchenker, and F. Louache. 2006. Reduced retention of radioprotective hematopoietic cells within the bone marrow microenvironment in CXCR4^{-/-} chimeric mice. *Blood* 107: 2243–2251.
54. Nie, Y., Y.-C. Han, and Y.-R. Zou. 2008. CXCR4 is required for the quiescence of primitive hematopoietic cells. *J. Exp. Med.* 205: 777–783.
55. Jung, P., C. Sommer, F. M. Barriga, S. J. Buczacki, X. Hernando-Momblona, M. Sevillano, M. Duran-Frigola, P. Aloy, M. Selbach, D. J. Winton, and E. Batlle. 2015. Isolation of Human Colon Stem Cells Using Surface Expression of PTK7. *Stem Cell Rep.* 5: 979–987.

Grant support:

ACL and MLA were supported by « Fondation pour la Recherche Médicale ». MDG was supported by la « Fondation de France ». The JPB's lab is supported by INSERM, Institut Paoli-Calmettes, and La Ligue Nationale Contre le Cancer ("Equipe labellisée"). The project was supported by INCa (Projet Libre INCa 2012-108 to MAL and JPB), SIRIC program (INCa-DGOS-Inserm 6038 to MAL and JPB) and Canceropole PACA (MAL, JPB). Jean-Paul Borg is a scholar of Institut Universitaire de France.

Figure Legends:

Figure 1: PTK7 expression in wild type bone marrow. (A) Expression of PTK7 in blood

mature cells. Granulocytes are defined as $\text{Gr1}^+\text{CD11b}^+$ cells. Monocytes are defined as $\text{F4/80}^+\text{CD11b}^+\text{CD115}^+$ cells. Lymphocytes are gated using B220, CD19, CD3, CD4 and CD8 combination. MFI ratios are indicated in dots plots. (B) Strategy of bone marrow progenitors gating. First panel: Dot plot showing the LSK^+ gate within Lin^- bone marrow cells. Second panel: dot plot showing early progenitors gating using SLAM markers. Hematopoietic stem cells (HSC) are defined as $\text{CD150}^+\text{CD48}^-$ cells. More mature multipotents progenitors (MPP) are defined as $\text{CD150}^+\text{CD48}^+$ (MPP2) and then $\text{CD150}^-\text{CD48}^+$ (MPP3/4). Third panel: dot plot showing engaged progenitors within $\text{c-Kit}^+\text{Sca-1}^-$ Lin^- cells. CMP (Common Myeloid Progenitor) is defined as $\text{CD16/32}^{\text{lo}}\text{CD34}^+$. GMP (Granulocyte-Macrophage Progenitor) is defined as $\text{CD34}^+\text{CD16/32}^{\text{hi}}$. MEP (Megakaryocyte-Erythroid Progenitor) is defined as $\text{CD16/32}^-\text{CD34}^-$. Fourth panel: Gating of CLP (Common Lymphoid Progenitor) defined as $\text{Lin}^-\text{IL7Ra}^+\text{B220}^-\text{CD24}^{\text{lo}}\text{CD117}^{\text{lo}}$. (C) Overlays showing expression of PTK7 during differentiation. Black line: PTK7, gray histogram: isotypic control (pre-immune rabbit antiserum). (D) Quantitative comparison of expression levels between different progenitor populations: normalization of PTK7 mean of fluorescence (MFO) with CD117 MFO on LSK subpopulations and progenitors ($\text{CD117}^+\text{Sca-1}^-$ cells). Statistical significance was calculated by nonparametric Mann-Whitney test. All data are shown as the mean \pm s.d. * $p < 0.05$. ** $p < 0.01$. *** $p < 0.001$.

Figure 2: Phenotype of PTK7 deficient mouse and analysis of fetal liver at E14.5. (A)

PTK7 mutants embryos showing severe planar cell polarity and developmental abnormalities. (B) Western blot of murine embryonic fibroblasts (MEFs) obtained from a

litter of our PTK7 gene trapped established mouse line. (C) Dot plots showing LSK gate within lin⁻ FL cells and SLAM gating within LSK cells. (D) Quantification of total number fetal liver cells. Data are pooled from 6 litters: *Ptk7*^{-/-} N=12; *Ptk7*^{+/-} N=19; *Ptk7*^{+/+} N=12 (E) Percentage of CD45⁺ cells within fetal liver. Data are pooled from 8 litters: *Ptk7*^{-/-} N=15; *Ptk7*^{+/-} N=26; *Ptk7*^{+/+} N=9. (F) Percentage of LSK cells within CD45⁺ FL cells. (G) Percentage of LSK subpopulation using SLAM markers. (H) Absolute number of LSK cells in E14.5 FL. (I) Absolute number of LSK subpopulations using SLAM markers. From (F) to (I) data are pooled from 10 litters: *Ptk7*^{-/-} N=19; *Ptk7*^{+/-} N=29; *Ptk7*^{+/+} N=10. (J) Survival curves of CD45.1 C57Bl/6 mice engrafted with 400 LSK cells sorted from CD45.2 FL together with 1.10⁵ congenic CD45.1 total bone marrow cells. Black line: engraftment with *Ptk7*^{+/+} FL cells; Dashed line: engraftment with *Ptk7*^{-/-} FL cells. Shown experiment is representative from 3 separate experiments. N=6 mice per group. (K) Clonogenic capacity of FL total cells. 3.10⁴ FL cells are seeded in M3434 methylcellulose. Shown experiment is representative from 3 separate experiments. *Ptk7*^{-/-} N=6; *Ptk7*^{+/+} N=4. All statistical significance was calculated by nonparametric Mann-Whitney test. All data are shown as the mean ± s.d. *p<0.05. **p<0.01. ***p<0.001.

Figure 3: Cell cycle and apoptosis analysis of LSK FL cells. (A) Representative dot plots of DNA content (DAPI) plotted versus Ki-67 nuclear antigen staining on LSK cells. The cell-cycle phases were defined as G0 (Ki-67⁻ and 2n DNA), G1(Ki-67⁺ and 2n DNA) and S-G2-M (Ki-67⁺ and DNA >2n). (B) Percentage of LSK FL cells in cell-cycle phases using SLAM markers. Data are pooled from 3 separate experiments and embryos (*Ptk7*^{-/-} N=10; *Ptk7*^{+/+} N=11) from 7 different litters. *p<0.05. **p<0.01. (C) Determination of percentage of apoptotic cells by staining with annexin V and DAPI. Apoptotic cells were defined as annexin V⁺ DAPI⁻. Results are representative of 8 *Ptk7*^{-/-} and 6 WT embryos from 5

different litters. All statistical significance was calculated by nonparametric Mann-Whitney test. All data are shown as the mean \pm s.d. * $p < 0.05$. ** $p < 0.01$. *** $p < 0.001$.

Figure 4: Hematological capacity of reconstitution and differentiation. Lethally irradiated CD45.1 mice (8 Gy) were reconstituted with 3.10^6 CD45.2 total FL cells isolated from $Ptk^{+/+}$ and $Ptk^{-/-}$ embryos. Percentage of each hematological populations from donor (CD45.2) was monitored by flow cytometry (A). Percentage of mature cells in recipient blood (B) and in spleen (C). Percentage of BM mature cells (D) and BM progenitors (E) in recipient mice. (F) Percentage of LSK cells and LSK subpopulation in recipient BM. White histograms depict mice reconstituted with $Ptk^{-/-}$ FL. Black histograms depict mice reconstituted with $Ptk^{+/+}$ FL. N=6 mice per group. (G) *In vitro* differentiation capacity of FL cells. 3.10^4 FL cells were seeded in methylcellulose. Left panel: Quantification and characterization of CFU-C. Right panel: Proportion of CFU. (H) Serial transplantation. First transplantation: Lethally irradiated mice were injected with 3.10^6 of total E14.5 FL cells (T1: transplantation 1). Next transplantations were done by injection of 3.10^6 total bone marrow cells from previously reconstituted mice in irradiated C57Bl/6 CD45.1 mice (T2 to T5). Percentage of donor cells (CD45.2) *versus* recipient cells (CD45.1) was monitored. Each data represents chimerism of definitive hematopoiesis 3 months after irradiation. Data are the mean \pm s.d. N=6 mice per group.

Figure 5: Competition experiments and cell cycle in adult mice. (A) 2.10^6 cells from $Ptk^{+/+}$ (CD45.1xCD45.2) and 2.10^6 cells from $Ptk^{-/-}$ (CD45.2) are injected in recipient (CD45.1) mice. Chimerism is followed in blood samples. Data are representative of 4 independent experiments (N=6 mice per group). (B-D) Recipient CD45.1 mice reconstituted with CD45.2 donor cells from wild type and mutant FL mice (B)

Representative dot plots of DNA contents (DAPI) plotted versus Ki-67 nuclear antigen staining on LSK cells. (C) Percentage of LSK cells in cell cycle phases using SLAM markers. (D) Clonogenic capacity of BM total cells. 1.10^5 BM cells are seeded in M3434 methylcellulose. Data are representative of 2 independent experiments (N=6 mice per group). All statistical significance was calculated by nonparametric Mann-Whitney test. * $p < 0.05$. ** $p < 0.01$. *** $p < 0.001$.

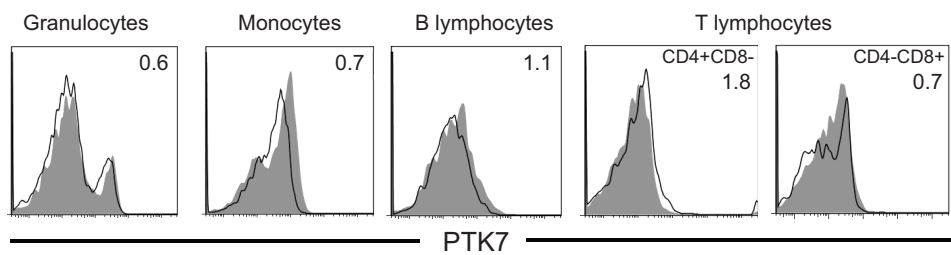
Figure 6: Homing capacities of deficient PTK7 cells. (A) 2.10^6 of total fetal liver cells from *Ptk7^{-/-}* or *Ptk7^{+/+}* embryos were stained with cell tracker calcein AM and calcein red-orange respectively, pooled in 1/1 ratio and injected in recipient mice. (B-D) 12h after injection, mice were sacrificed and biological samples were removed and analyzed to evaluate homing capacities of each cells. (B) Bone marrow of uninjected mice was used as control for staining specificity. (C) Dot plots of stained cells removed from blood, BM, spleen, liver and thymus. (D) Quantification and statistical analysis. Data are pooled from 3 independent experiments or representative (for spleen panel). N=6 mice per group. All statistical significance was calculated by nonparametric Mann-Wihtney test. * $p < 0.05$. ** $p < 0.01$. *** $p < 0.001$.

Figure 7: Adhesion and migration assays (A). Adhesion assay on MS5 stromal cells. Percentage of adherent FL cells on MS5 stromal bone marrow cell line after 2 hours of incubation. Left panel: total FL cells. Right panel: LSK cells. Data are representative of 3 independent experiments. *Ptk^{-/-}* N=4; *Ptk^{+/-}* N=6; *Ptk^{+/+}* N=3. (B to E) Migration in Boyden chamber assay. Number of migrating cells are normalized to the number of input cells for each sample (duplicate wells). (B) Migration of lin^{Neg} enriched FL cells without chemoattractant. (C) Migration of lin^{Neg} enriched FL cells with SDF1a as chemoattracting

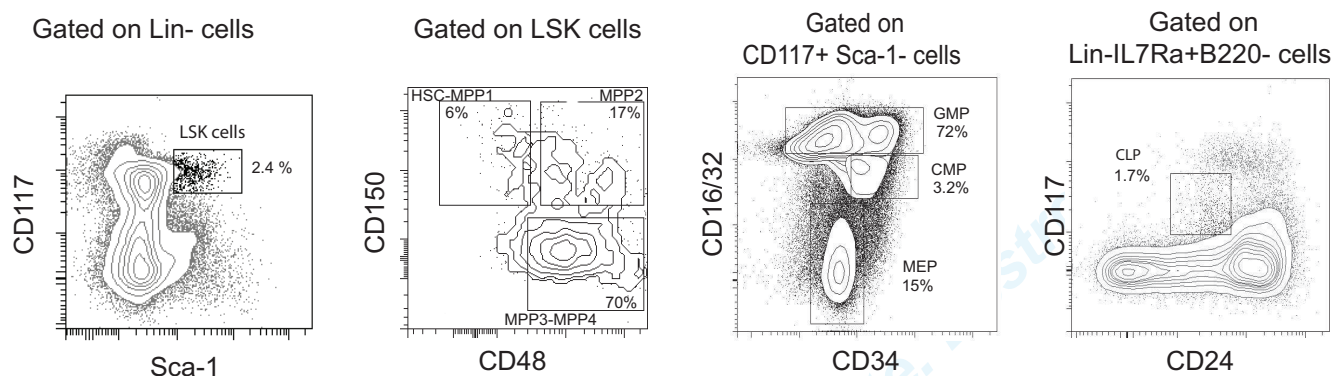
794 reagent. (D). Migration of LSK FL cells without chemoattractant. (E). Migration of LSK
795 FL cells with SDF1 α as chemoattracting reagent. All statistical significance was calculated
796 by nonparametric Mann-Wihtney test. *p<0.05. **p<0.01. ***p<0.001.

For Peer Review. Do not distribute. Destroy after use.

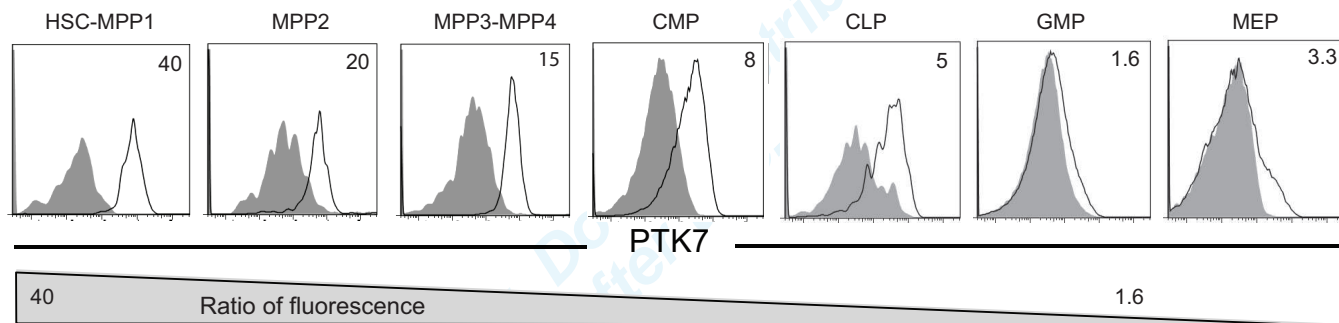
A.



B.



C.



D.

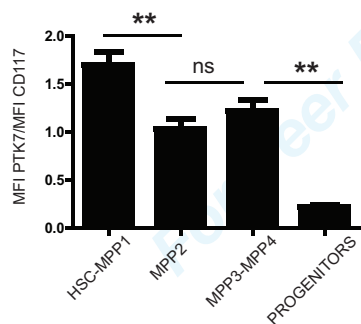


Figure 1

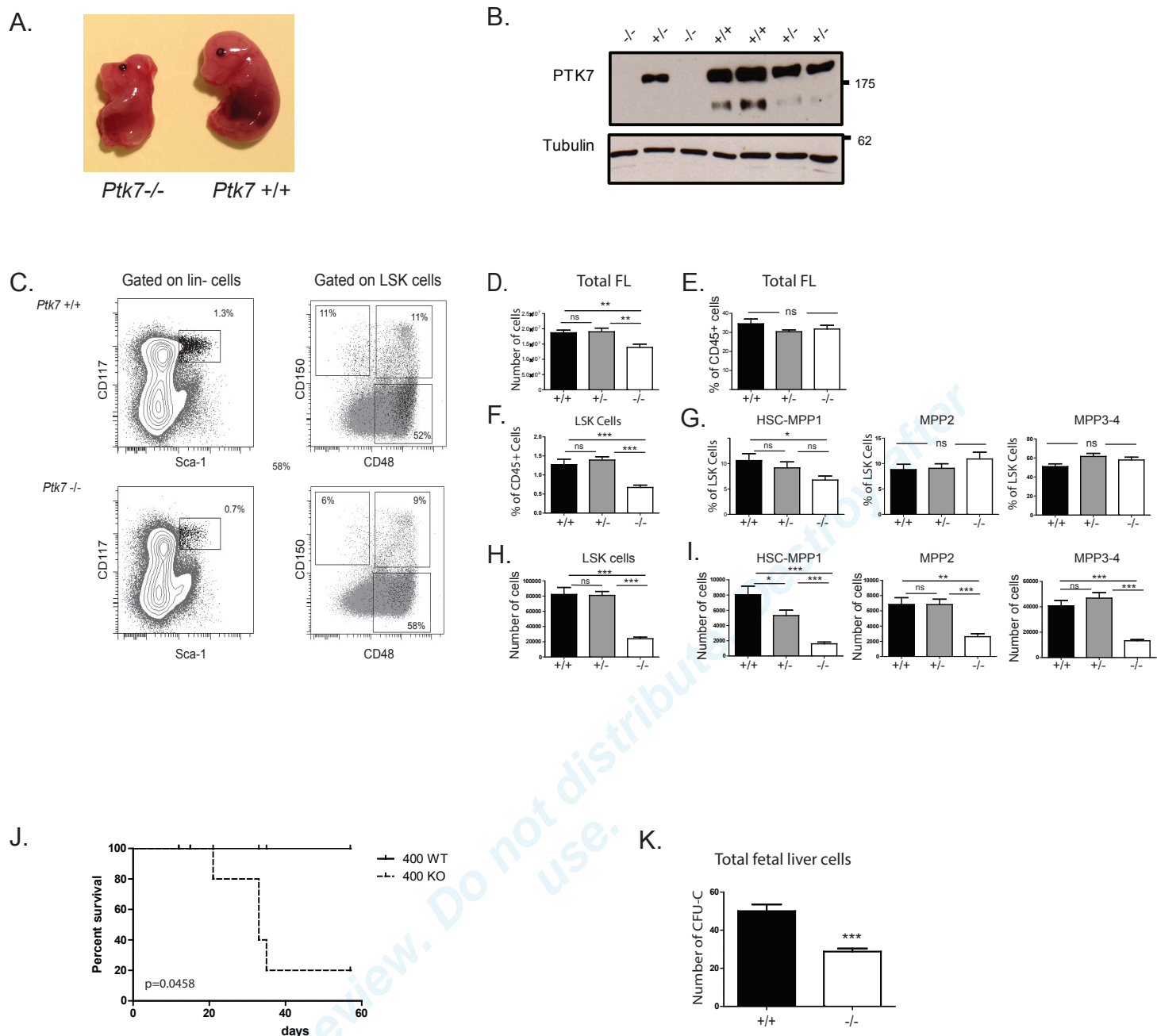


Figure 2

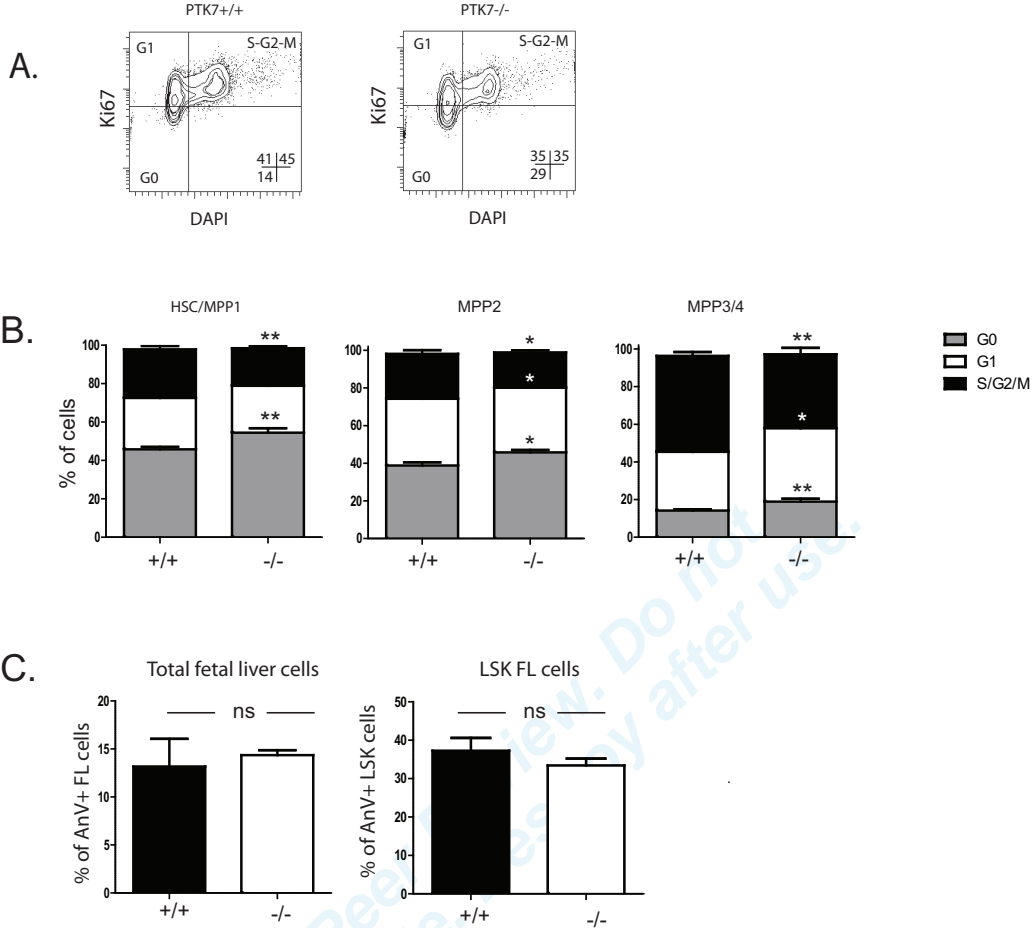


Figure 3

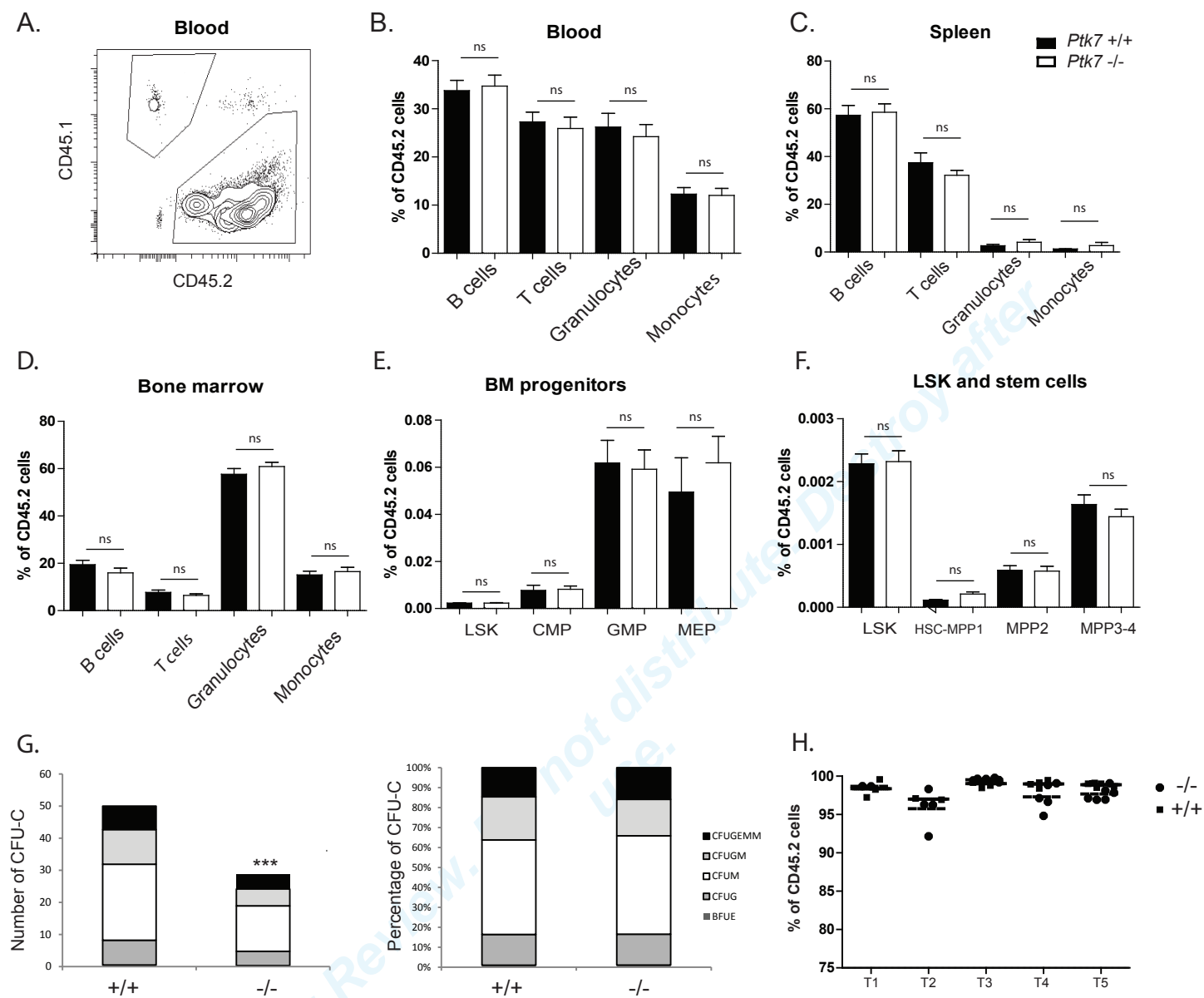
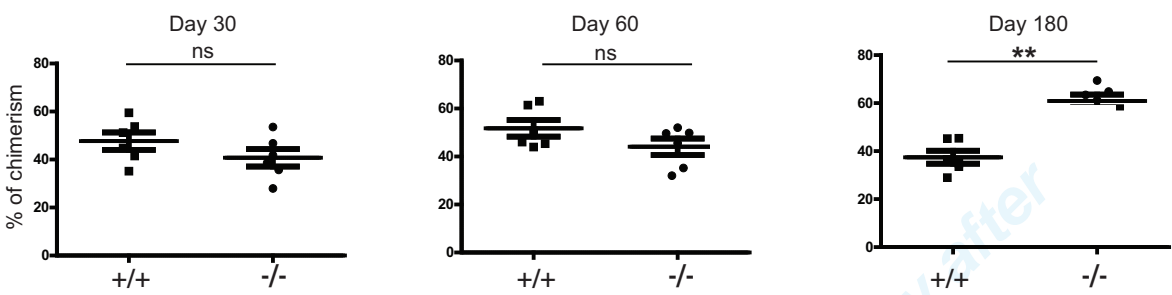
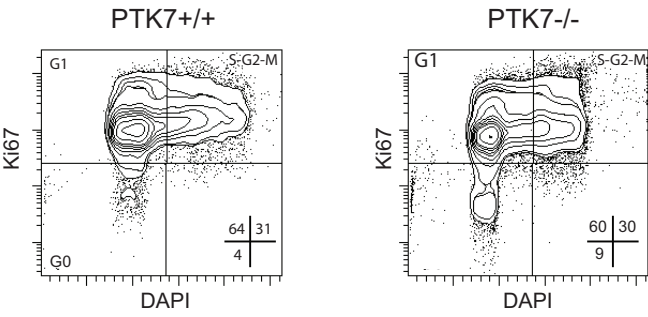


Figure 4

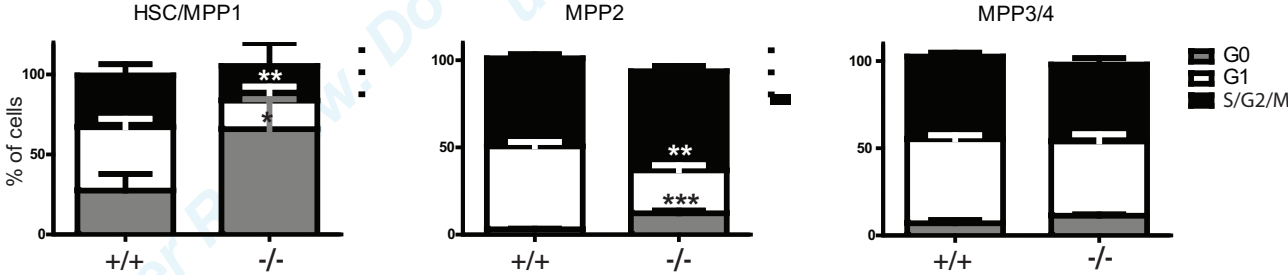
A.



B.



C.



D.

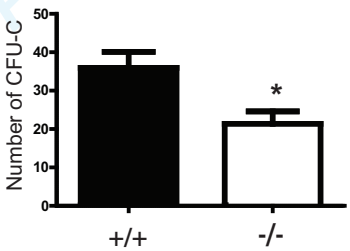


Figure 5

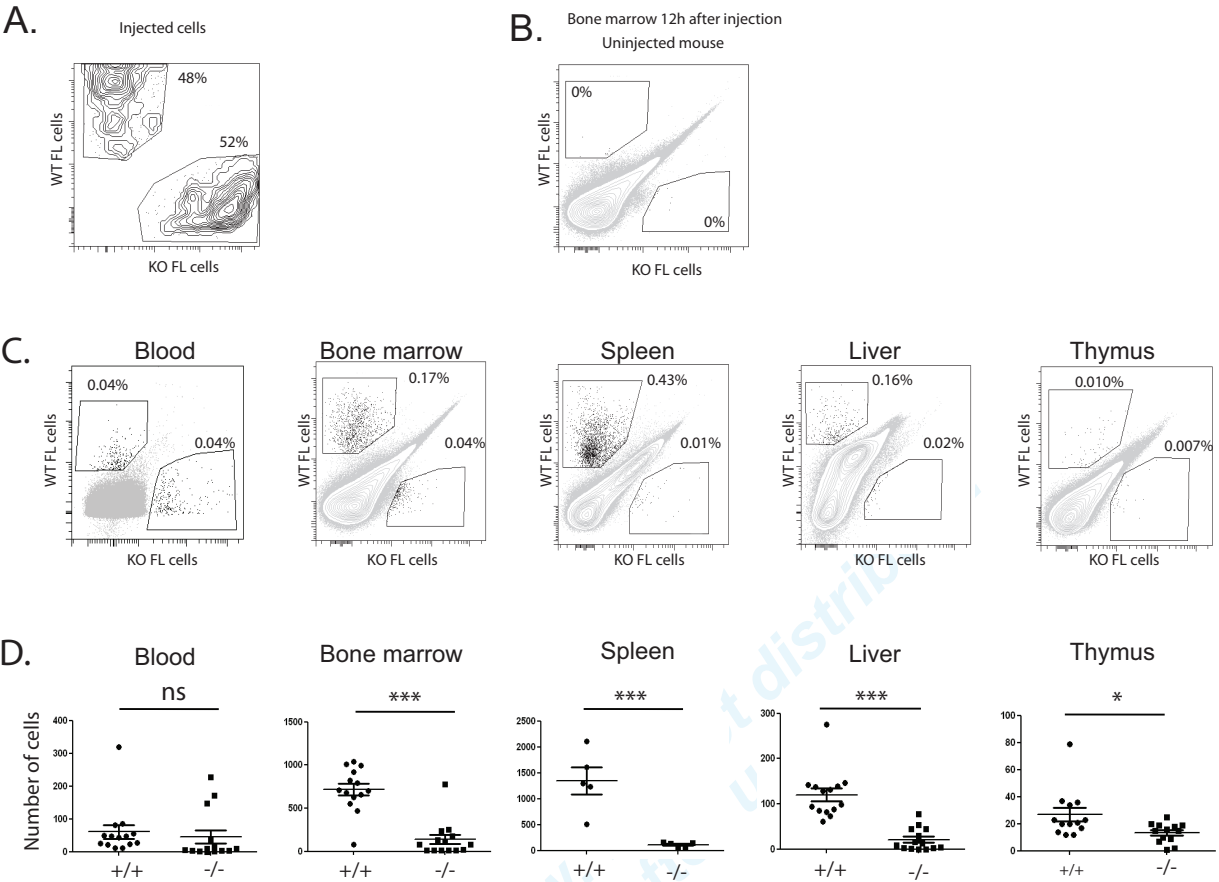


Figure 6

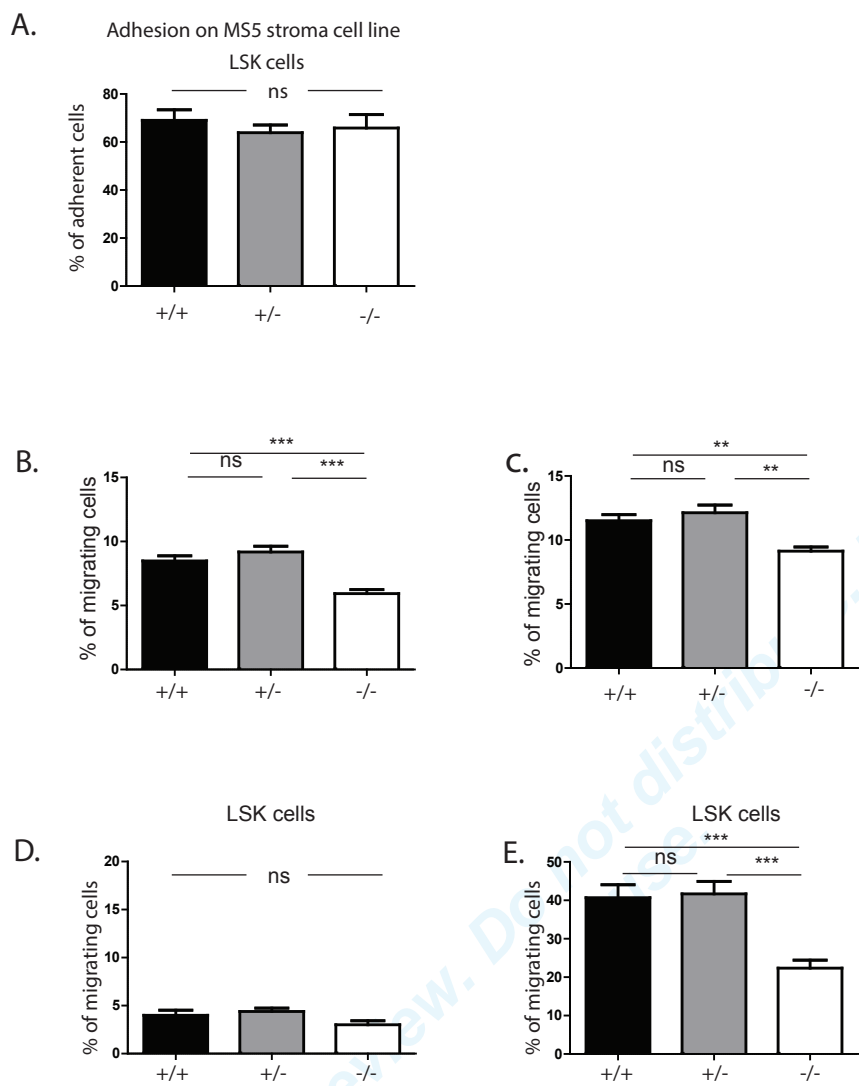


Figure 7